

Zr–Al–Ni–Cu glass forming alloys with low fragility parameters

Wei-ke AN¹, Xiang XIONG², Yong LIU², An-hui CAI^{1,2}, Guo-jun ZHOU¹, Yun LUO¹, Tie-lin LI¹, Xiao-song LI¹

1. College of Mechanical Engineering, Hunan Institute of Science and Technology, Yueyang 414006, China;

2. State Key Laboratory of Powder Metallurgy, Central South University, Changsha 410083, China

Received 3 December 2012; accepted 17 June 2013

Abstract: Zr–Al–Ni–Cu bulk metallic glasses (BMGs) were developed and their fragility parameters (m) were calculated by Arrhenius and Vogel–Fulcher–Tammann (VFT) equations. The results show that the m values of the Zr–Al–Ni–Cu BMGs derived by Arrhenius equation are in agreement with the corresponding m values derived by VFT equation. These Zr–Al–Ni–Cu BMGs characterize in low m values. The low m values for these BMGs would be due to their network microstructures. In addition, the m values of Zr–Al–Cu–Ni BMGs could be obtained by regulating Zr content. The composition of Zr–Al–Cu–Ni BMGs with the lowest m value would be near 54%Zr (mole fraction) because the m value about 13 of $Zr_{54}Al_{13}Cu_{18}Ni_{15}$ BMG is the lowest among these Zr–Al–Ni–Cu BMGs developed.

Key words: Zr–Al–Ni–Cu alloy; metallic glass; fragility

1 Introduction

Up to now, many kinds of bulk metallic glasses have been developed including Mg-, La-, Zr-, Ti-, Cu-, Nd-, Fe-, Pr-, Pd-, Ce-, Ca-, and other rare earth-based [1–5]. Among them, Zr-based bulk metallic glasses can be produced by the conventional casting process, leading to successful applications as sporting goods, surgical instruments and electronic devices. The applications of metallic glasses require high stability in various environments in order to ensure an acceptable lifetime. The metallic glasses are metastable materials. With increase of temperature, such non-crystalline systems transform into crystalline state in course of time. From the technological application point of view, the thermal stability of the metallic glasses is of considerable importance. The fragility parameter m can be used to estimate the thermal stability and/or glass forming ability (GFA) of metallic glass. In addition, the m has been used to segregate glass forming materials into three general categories: strong, intermediate and fragile liquids [6,7]. For strong liquids, m is less than 30 with a lower limit of about 16. For example, the rigid tetrahedral network oxides SiO_2 and GeO_2 have m value of 20 at glass

transition temperature T_g [7]. In contrast, fragile liquids such as polymers and ionic melts which have thermally sensitive structures that can be easily disrupted by small increase in temperature display large values of $m \geq 100$. In the case of metallic glasses, a previous compilation of the m for a range of ternary and higher-order alloys indicated an intermediate fragility strength where $30 < m < 70$ [8], such as Zr- ($m=34-39$), Fe- ($m=34$), and Pd-based ($m=41$) BMGs [9]. However, ZHANG et al [3] found that the m value of $Ce_{60}Ni_{10}Al_{10}Cu_{20}$ BMG was 21, which was the lowest m value for metallic glasses. Then, could other BMGs with lower m value than 21 be developed?

In the present work, a family of BMGs consisting of conventional metallic components Zr, Al, Ni, and Cu was obtained. Through compositional modification, Zr–Al–Ni–Cu ternary BMGs with relative low m values, even lower than 16 were developed.

2 Experimental

2.1 Composition design

CHEN et al [10] noticed that the known amorphous phases in Zr–Al–Ni, Zr–Al–Cu, and Zr–Al–Ni–Cu systems all have $e/a = \sum C_i E_i$ (C_i and E_i are atomic fraction

Foundation item: Project (50874045) supported by the National Natural Science Foundation of China; Projects (200902472, 20080431021) supported by the China Postdoctoral Science Foundation; Project (10A044) supported by the Research Foundation of Education Bureau of Hunan Province of China

Corresponding author: An-hui CAI; Tel: +86-730-8648848; E-mail: cah1970@sohu.com

DOI: 10.1016/S1003-6326(13)62869-1

and conduction electron concentration of the i th element, respectively) ratios in the range of 1.3–1.5 close to the value of 1.4 of Inoue alloy and average atomic radius $R_a = \sum C_i R_i$ (R_i is atomic radius of the i th element) in the range of 0.1487–0.1533 nm close to 0.1496 nm of Inoue alloy. They determined that the conduction electron concentrations for Zr, Al, Ni and Cu are 1.5, 3, 0, and 1.0, respectively. Then a group of Zr–Al–Ni–Cu glass forming alloys was designed by $e/a=1.4$, $R_a=0.1496$ nm, and $\sum C_i=1$ by adding a suitable cluster. However, it is difficult for selecting a suitable cluster in multi-component alloys. A large quantity of direct and indirect evidence [11–16] shows topological and chemical short-range order (SRO) in amorphous alloy. Compositional difference, even minor addition can change the magnitude, type and distribution of SRO [14,15], which influences the relaxation, diffusion and rearrangement of atoms, resulting in the change of GFA and thermal stability of glass forming alloys [16]. In addition, better GFA and thermal stability of glass forming alloy are achieved for the rationalization of the combination of the magnitude, type and distribution of SRO [16]. The microstructure of metallic glass inherits from the melt. The magnitude, category, and stability of SRO are related with the binding force among atoms. It is well known that the melting heat ΔH_m can be used to characterize the binding force. In addition, we found that the Zr–Al–Ni–Cu system had optimum GFA when the melting heat $\Delta H_m = \sum C_i \Delta H_{mi}$ (ΔH_{mi} is the melting heat of the i th element) was near 19.7146 kJ/mol [17]. A group of Zr–Al–Ni–Cu glass forming alloys is designed by merging the ΔH_m condition with three afore-mentioned conditions. It must be noticed that the ΔH_m constraint condition is not strong but weak. If the ΔH_m constraint condition is strong, the composition is unique. On the other hand, if the ΔH_m constraint condition is weak, there are many finite compositions satisfying with four

conditions. The constraint conditions for Zr–Al–Ni–Cu glass forming alloys are: $e/a=1.38$, $d_a=0.1500$ nm and $\Delta H_m \approx 19$ kJ/mol for $Zr_{54}Al_{13}Cu_{18}Ni_{15}$; $e/a=1.38$, $d_a=0.1486$ nm and $\Delta H_m \approx 19.7$ kJ/mol for other Zr–Al–Ni–Cu alloys. The detailed compositions for Zr–Al–Ni–Cu alloys are listed in Table 1.

2.2 Experimental procedures

Pre-alloyed Zr–Al–Ni–Cu ingots with nominal compositions (mole fraction, %), as shown in Table 1, were prepared by arc melting of the pure elements: Zr (99.99%), Ni (99.99%), Cu (99.99%), and Al (99.99%) under a Ti-gettered argon atmosphere. The ingots were remelted five times in order to obtain homogeneity and finally cylindrical rods with 2 mm in diameter were prepared from the pre-alloyed ingots by suction casting into a water-cooled copper mould.

2.3 Testing methods

The structure of the as-cast samples was characterized by X-ray diffraction (XRD) using an XD-3A diffractometer with Cu K_α and transmission electron microscopy (TEM) using a JEM2000EX instrument operated at 160 kV, respectively. The microstructure was investigated by an SIRION scanning electronic microscope (SEM) operated at 20 kV. The energy dispersive spectrometry (EDS) system was combined with the TEM. The microhardness was performed using an HVI-10A microhardness tester under a load of 1.47 kN for a dwell time of 30 s. Thermal analysis was carried out using DSC-404C differential scanning calorimeter at heating rates of 0.25, 0.33, 0.5 and 0.67 ks^{-1} , respectively.

3 Results and discussion

Figure 1 shows that these glass forming alloys can

Table 1 Glass transition temperature T_g , undercooled liquid region ΔT_x , fragility parameters m_A and m_v for Zr-based metallic glasses

Metallic glass	T_g/K				$\Delta T_x/K$	m_A	m_v
	0.25 ks^{-1}	0.33 ks^{-1}	0.5 ks^{-1}	0.67 ks^{-1}			
$Zr_{65}Al_{8.7}Cu_{14.4}Ni_{11.9}$	647.0	648.0	652.7	655.3	69.9	30.1	35.2
$Zr_{64}Al_{10.1}Cu_{11.7}Ni_{14.2}$	657.9	662.8	668.5	672.0	60.8	20.3	18.3
$Zr_{63.5}Al_{10.7}Cu_{10.7}Ni_{15.1}$	653.5	658.6	667.1	669.6	71.9	16.7	17.2
$Zr_{62.5}Al_{12.1}Cu_{7.95}Ni_{17.45}$	668.9	672.5	679.1	688.8	68.9	13.6	23.5
$Zr_{62}Al_{10}Cu_{15}Ni_{13}$	660.6	661.8	669.3	674.7	75.5	17.8	25.8
$Zr_{61.5}Al_{10.7}Cu_{13.65}Ni_{14.15}$	664.2	670.1	675.2	681.1	67.4	16.7	15.8
$Zr_{60.5}Al_{12.1}Cu_{10.95}Ni_{16.45}$	681.4	685.2	688.3	692.3	70.1	27.0	26.4
$Zr_{54}Al_{13}Cu_{18}Ni_{15}$	700.6	709.2	717.2	720.3	71.0	14.1	12.9
$Zr_{41}Ti_{14}Ni_{10}Cu_{12.5}Be_{22.5}$					57 [18,19]		39 [20]
$Zr_{65}Cu_{17.5}Ni_{10}Al_{7.5}$					79.1 [21,22]		35 [23]
$Zr_{65}Al_{10}Ni_{10}Cu_{15}$					79.5 [5,24]		35 [5]

be cast into entirely glassy rods with diameter of 2 mm without any apparent crystalline Bragg peaks. Clear glass transitions and sharp crystallization events are observed in the DSC traces (Fig. 2), confirming the glassy nature of these BMGs. The thermal parameters are also summarized in Table 1.

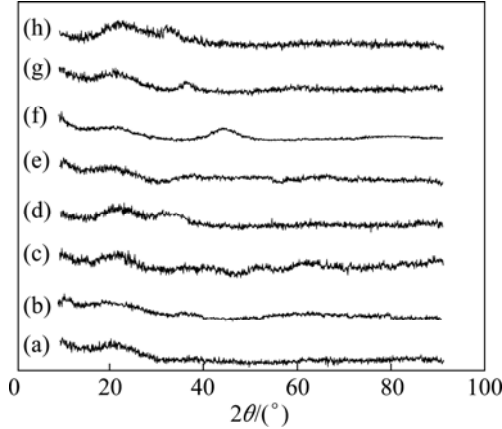


Fig. 1 XRD patterns for Zr–Al–Ni–Cu glass forming alloys: (a) $Zr_{54}Al_{13}Cu_{18}Ni_{15}$; (b) $Zr_{60.5}Al_{12.1}Cu_{10.95}Ni_{16.45}$; (c) $Zr_{61.5}Al_{10.7}Cu_{13.65}Ni_{14.15}$; (d) $Zr_{62}Al_{10}Cu_{15}Ni_{13}$; (e) $Zr_{62.5}Al_{12.1}Cu_{7.95}Ni_{17.45}$; (f) $Zr_{63.5}Al_{10.7}Cu_{10.7}Ni_{15.1}$; (g) $Zr_{64}Al_{10.1}Cu_{11.7}Ni_{14.2}$; (h) $Zr_{65}Al_{8.7}Cu_{14.4}Ni_{11.9}$

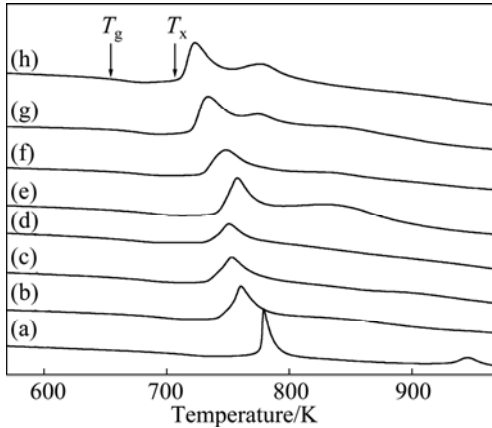


Fig. 2 DSC curves for Zr–Al–Ni–Cu glass forming alloys: (a) $Zr_{54}Al_{13}Cu_{18}Ni_{15}$; (b) $Zr_{60.5}Al_{12.1}Cu_{10.95}Ni_{16.45}$; (c) $Zr_{61.5}Al_{10.7}Cu_{13.65}Ni_{14.15}$; (d) $Zr_{62}Al_{10}Cu_{15}Ni_{13}$; (e) $Zr_{62.5}Al_{12.1}Cu_{7.95}Ni_{17.45}$; (f) $Zr_{63.5}Al_{10.7}Cu_{10.7}Ni_{15.1}$; (g) $Zr_{64}Al_{10.1}Cu_{11.7}Ni_{14.2}$; (h) $Zr_{65}Al_{8.7}Cu_{14.4}Ni_{11.9}$

For glass forming liquids, the temperature dependence of η on the temperature intervals between T_m and T_g can be described by the Vogel–Fulcher–Tammann (VFT) equation [25]:

$$\eta = \eta_0 \exp\left(\frac{B}{T - T_0}\right) \quad (1)$$

where η_0 , B and T_0 are fitting parameters and T is the temperature. Often over a narrower temperature range,

especially near T_g , $\eta(T)$ can also be approximated very well by an Arrhenius equation where $T_0=0$ in Eq. (1), and is given by

$$\eta = \eta_0 \exp\left(\frac{E_a}{RT}\right) \quad (2)$$

where E_a is an activation energy and R is the gas mole constant.

For some liquids, such as SiO_2 and GeO_2 which have a three-dimensional tetrahedral network structure, the Arrhenius law can be used to fit $\eta(T)$ over the entire temperature range between T_m and T_g [26]. All other glass forming liquids exhibit varying degrees of departure from Arrhenius behavior. Strong liquids are those with an Arrhenius temperature dependent of the viscosity, while fragile liquids are more sensitive to thermal changes and display large deviations from Arrhenius behavior. In order to quantify the fragility (the degree of departure from an Arrhenius temperature dependence), BÖHMER et al [6,27] introduced a fragility parameter m defined as

$$m = \frac{d \lg \tau(T)}{dT_g / T} \Big|_{T=T_g} \quad (3)$$

where $\tau(T)$ is relaxation time. Since the viscosity is proportional to a structural relaxation time, m can be estimated by replacing $\tau(T)$ with $\eta(T)$ in Eq. (3). The fragility parameter m is then a measure of the steepness of the slope of the viscosity curve at T_g when the temperature is scaled by T_g . If $\eta(T)$ can be described by the Arrhenius equation, then,

$$m = \frac{E_g}{RT_g \ln 10} \quad (4)$$

On the other hand, values of fragility can be directly taken by the VFT equation fitting to viscosity data [7]. The liquid fragility can be determined from a purely thermodynamic way near T_g , and the m estimated by this method is consistent with that obtained by the kinetic method [28]. Since viscosity relaxation and the glass transition measured by calorimetric methods occur on the same time scale, the dependence of heating rate β on glass transition can be used as an alternative way to determine the fragility of the glasses [3,28–34]. Previous studies confirm that the β dependent on T_g describes the fragility equally well as complementary viscosity measurements [31]. Therefore, the dependence of T_g on β can also be described by a VFT-type relation:

$$\beta(T_g) = A \exp[D^* T_g^0 / (T_g^0 - T_g)] \quad (5)$$

where A is a constant, T_g^0 is the VFT temperature, and D^* is the strength parameter. From the relationship

between T_g and β of the metallic glasses using the VFT equation, the VFT parameters A , T_g^0 , and D^* are obtained. Then m can be obtained as

$$m = (D^* / \ln 10) (T_g^0 / T_g) (1 - T_g^0 / T_g)^{-2} \quad (6)$$

Although the uncertainty of the values of T_g^0 and D^* is quite large, the change of T_g^0 results in change of D^* , which keeps the m value reasonably constant [28–33]. The relationship between T_g and β was fitted with the VFT equation. From the best fit according to Eqs. (5) and (6), the m values (m_v) for Zr–Al–Cu–Ni are shown in Table 1. On the other hand, the m values (m_A) calculated by Eq. (4) at the heating rate of 0.33 ks^{-1} are also listed in Table 1. Obviously, the m_A and m_v values are consistent with each other although the m_A deviates from the m_v for $\text{Zr}_{62.5}\text{Al}_{12.1}\text{Cu}_{7.95}\text{Ni}_{17.45}$. In addition, the m_v values for these Zr–Al–Ni–Cu BMGs are less than 36. Among them, the m_v values for $\text{Zr}_{54}\text{Al}_{13}\text{Cu}_{18}\text{Ni}_{15}$, $\text{Zr}_{61.5}\text{Al}_{10.7}\text{Cu}_{13.65}\text{Ni}_{14.15}$, $\text{Zr}_{64}\text{Al}_{10.1}\text{Cu}_{11.7}\text{Ni}_{14.2}$ and $\text{Zr}_{63.5}\text{Al}_{10.7}\text{Cu}_{10.7}\text{Ni}_{15.1}$ BMGs are less than 20. Especially, the m_v values for $\text{Zr}_{54}\text{Al}_{13}\text{Cu}_{18}\text{Ni}_{15}$ and $\text{Zr}_{61.5}\text{Al}_{10.7}\text{Cu}_{13.65}\text{Ni}_{14.15}$ BMGs are less than 16. This indicates that these Zr–Al–Ni–Cu BMGs have the similar microstructure to SiO_2 and GeO_2 . As shown in Fig. 1, a high halo about $2\theta=20^\circ$ appears which is smaller than that of other Zr–Al–Ni–Cu metallic glasses ($2\theta=40\text{--}50^\circ$) [10,14,15,32,18–20,23]. If the average distance d between the atoms is estimated by

$$d = \frac{\lambda}{2 \sin \theta} \quad (7)$$

where θ and λ are angle and wavelength of incident ray, respectively. Then, the d values of the studied Zr–Al–Ni–Cu metallic glasses are about 2 times those of other Zr–Al–Ni–Cu metallic glasses. This indicates that the size of the short and/or medium range orders of studied Zr–Al–Ni–Cu metallic glasses is 2 times larger than other Zr–Al–Ni–Cu metallic glasses, resulting in that these orders can be observed. Thus the cross-sections of all Zr–Al–Ni–Cu metallographic specimens are etched with 20% hydrofluoric acid solution. Figure 3(a) shows a typical microstructure of $\text{Zr}_{61.5}\text{Al}_{10.7}\text{Cu}_{13.65}\text{Ni}_{14.15}$ metallic glass. We can clearly observe a network structure which is due to not the corrosive cracking but the dissolution of the alloy elements because no cracks are observed (see Figs. 3(b) and (c)). In addition, we can clearly observe from Figs. 4(a) and (c) that the network structure does not show the characteristics of the crack. Microhardness tests are conducted on the “matrix” and vicinity of the “network”, as shown in Figs. 3(b) and (c). The different hardnesses are clearly seen from the different sizes of two indentations. It would be due to the different

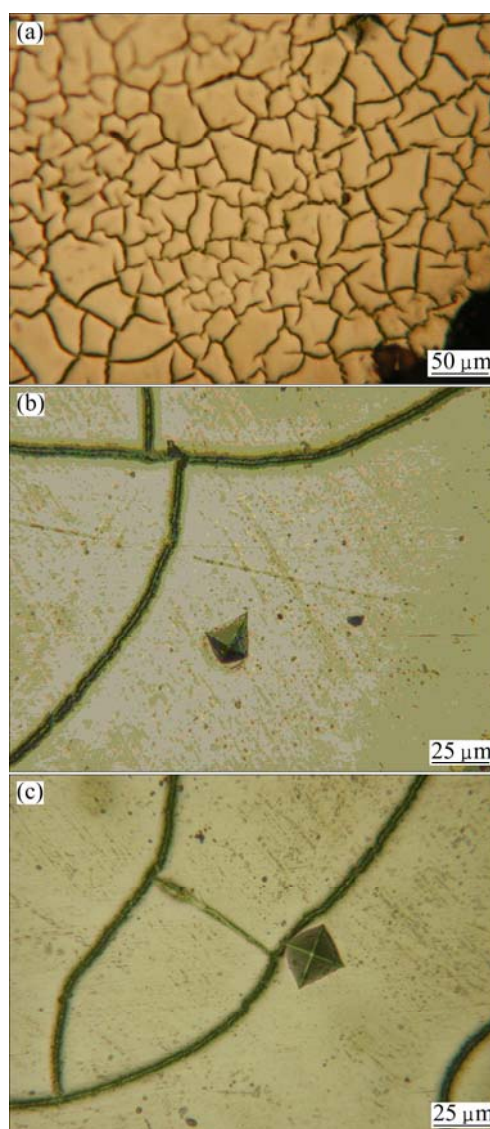


Fig. 3 Typical network-like microstructure (a) and indentation of $\text{Zr}_{61.5}\text{Al}_{10.7}\text{Cu}_{13.65}\text{Ni}_{14.15}$ metallic glass (b, c)

contents of the alloying elements, resulting in the different corrosion resistances and different dissolution rates.

The selected-area electron diffraction SAED patterns (the inset of Figs. 4(a) and (b)) for $\text{Zr}_{61.5}\text{Al}_{10.7}\text{Cu}_{13.65}\text{Ni}_{14.15}$ indicate the amorphous states not only for the matrixes but also for the networks without the observation of the diffraction dots for the crystalline phase.

As shown in Figs. 4(c) and (d), although the number of elements is the same for the matrix and the network, the content of alloy elements for the matrix is different from that for the network. The difference of the content of alloy elements is the largest for Zr, namely, the content of Zr is more in the matrix than in the network, resulting in the difference of the corrosion resistance between the matrix and the network. It is also indirectly proved by different hardnesses, as shown in Figs. 3(b)

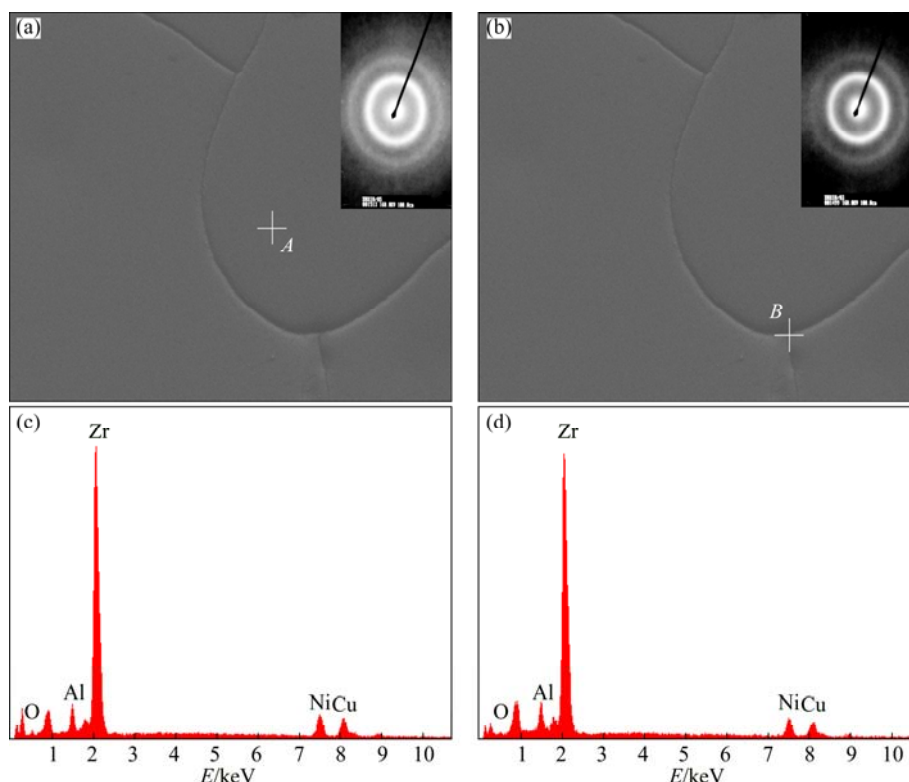


Fig. 4 SEM images (a, b) and EDS results for areas *A* (c) and *B* (d) of $Zr_{61.5}Al_{10.7}Cu_{13.65}Ni_{14.15}$ metallic glass (The insets are selected-area electron diffraction patterns of *A* (a) and selected-area electron diffraction pattern for *B* (b), respectively)

and (c). Recently, LIU et al [35] found that the size and distribution of *B2* CuZr particles can be effectively homogenized by Ta addition in rapidly solidified $Cu_{47}Zr_{48-x}Al_5Ta_x$ ($0 \leq x \leq 1\%$, mole fraction) alloys. This indicates that a regular distribution of the alloying elements appears when the content of the alloying elements arrives at a rational value. Thus, the network structure results in a lower *m* for Zr–Al–Ni–Cu BMGs investigated. The small value of *m* is considered to be one of the empirical rules for designing the BMG formers whose metastable-equilibrium supercooled liquid is fairly stable [32]. The afore-mentioned results indicate the better GFA [17,36] and thermal stability for the investigated Zr–Al–Ni–Cu BMGs. As shown in Table 1, the undercooled liquid region ΔT_x of the investigated Zr–Al–Ni–Cu BMGs is more than that of $Zr_{41}Ti_{14}Ni_{10}Cu_{12.5}Be_{22.5}$ [18,19], and the *m* of the former is smaller than that of the latter, indicating that the thermal stability of the former is better than that of the latter. In addition, we compared the investigated Zr–Al–Ni–Cu BMGs with other Zr-based BMGs [5,23,20], as shown in Table 1. One can observe that the *m* value of Zr–Al–(Cu, Ni) BMGs is the same when Zr content is 65%. Otherwise, the *m* value of Zr–Al–(Cu, Ni) BMGs less than 65% Zr is smaller than that of Zr–Al–(Cu, Ni) BMGs with 65% Zr. Especially, the *m* decreases down to the smallest when the Zr content decreases down to 54%. This indicates that

Zr–Al–(Cu, Ni) BMGs with the low *m* could be obtained by regulating the Zr content and the composition of Zr–Al–(Cu, Ni) BMGs with the lowest *m* is near 54%Zr. These phenomena are necessary for further investigation.

4 Conclusions

1) A series of Zr–Al–Ni–Cu BMGs are developed and characterized in low fragility parameter values. The fragility parameter values of these BMGs are between 13 and 36.

2) The low fragility parameter values of these BMGs would be due to their network microstructures. Zr–Al–Cu–Ni BMGs with the low fragility parameter values could be obtained by regulating the Zr content. The composition of Zr–Al–Cu–Ni BMGs with the lowest fragility parameter value is near 54%Zr.

References

- [1] KHADEMIAN N, GHOLAMIPOUR R. Effects of infiltration parameters on mechanical and microstructural properties of tungsten wire reinforced $Cu_{47}Ti_{33}Zr_{11}Ni_6Sn_2Si_1$ metallic glass matrix composites [J]. Transactions of Nonferrous Metals Society of China, 2013, 23: 1314–1321.
- [2] CAI An-hui, XIONG Xiang, LIU Yong, AN Wei-ke, ZHOU Guo-jun, LUO Yun, LI Tie-lin, LI Xiao-song. A Cu-based bulk amorphous composite reinforced by carbon nanotube [J]. Transactions of Nonferrous Metals Society of China, 2012, 22(9): 2191–2197.

- [3] ZHANG B, WANG R J, ZHAO D Q, PAN M X, WANG W H. Properties of Ce-based bulk metallic glass-forming alloys [J]. Phys Rev B, 2004, 70: 224208.
- [4] WANG W H. Roles of minor additions in formation and properties of bulk metallic glasses [J]. Prog Mater Sci, 2007, 52: 540–596.
- [5] WANG W H, DONG C, SHEK C H. Bulk metallic glasses [J]. Mater Sci Eng R, 2004, 44: 45–89.
- [6] BÖHMER R, NGAI K L, ANGELL C A, PLAZEK D J. Nonexponential relaxations in strong and fragile glass formers [J]. J Chem Phys, 1993, 99: 4201–4209.
- [7] ANGELL C A. Formation of glasses from liquids and biopolymers [J]. Science, 1995, 267: 1924–1935.
- [8] PERERA D N. Compilation of the fragility parameters for several glass-forming metallic alloys [J]. J Phys: Condens Mater, 1999, 11: 3807–3812.
- [9] WANG W H. Correlations between elastic moduli and properties in bulk metallic glasses [J]. J Appl Phys, 2006, 99: 093506.
- [10] CHEN W, WANG Y, QIANG J, DONG C. Bulk metallic glasses in the Zr–Al–Ni–Cu system [J]. Acta Mater, 2003, 51: 1899–1907.
- [11] CHEN G L, HHUI X D, FAN S W, KOU H C, YAO K F. Concept of chemical short range order domain and the glass forming ability in multicomponent liquid [J]. Intermetallics, 2002, 10: 1221–1232.
- [12] DOVE J P K, MEYER L. Mapping the magic numbers in binary Lennard-Jones clusters [J]. Phys Rev Lett, 2005, 95: 063401.
- [13] HUFNAGEL T C, BRENNAN S. Short- and medium-range order in (Zr₇₀Cu₂₀Ni₁₀)_{90-x}Ta_xAl₁₀ bulk amorphous alloys [J]. Phys Rev B, 2003, 67: 014203.
- [14] LUO W K, SHENG H W, ALAMGIR F M, BAI J M, HE J H, MA E. Icosahedral short-range order in amorphous alloys [J]. Phys Rev Lett, 2004, 92: 145502.
- [15] SAIDA J, INOUE A. Icosahedral quasicrystalline phase formation in Zr–Al–Ni–Cu glassy alloys by the addition of V, Nb and Ta [J]. J Non-Cryst Solids, 2002, 312–314: 502–507.
- [16] KO H S, CHANG J Y. Effect of short-range order in liquid on the glass forming ability of Fe–Si–B alloy wires [J]. Mater Lett, 2004, 58: 1012–1016.
- [17] CAI A H, CHEN H, AN W K, TAN J Y, ZHOU Y. Relationship between melting enthalpy ΔH_m and critical cooling rate R_c for bulk metallic glasses [J]. Mater Sci Eng A, 2007, 457: 6–12.
- [18] BUSCH R, KIM Y J, JOHNSON W L. Thermodynamics and kinetics of the undercooled liquid and the glass transition of the Zr_{41.2}Ti_{13.8}Cu_{12.5}Ni_{10.0}Be_{22.5} alloy [J]. J Appl Phys, 1995, 77: 4039–4044.
- [19] BUSCH R, JOHNSON W L. The kinetic glass transition of the Zr_{46.75}Ti_{8.25}Cu_{7.5}Ni₁₀Be_{27.5} bulk metallic glass former-supercooled liquids on a long time scale [J]. Appl Phys Lett, 1998, 72: 2695–2697.
- [20] WANIUK T A, BUSCH R, MASUHR A, JOHNSON W L. Equilibrium viscosity of the Zr_{41.2}Ti_{13.8}Cu_{12.5}Ni₁₀Be_{22.5} bulk metallic glass-forming liquid and viscous flow during relaxation, phase separation, and primary crystallization [J]. Acta Mater, 1998, 46: 5229–5236.
- [21] LU Z P, TAN H, LI Y, NG S C. The correlation between reduced glass transition temperature and glass forming ability of bulk metallic glasses [J]. Scripta Mater, 2000, 42: 667–673.
- [22] LU Z P, LI Y, NG S C. Reduced glass transition temperature and glass forming ability of bulk glass forming alloys [J]. J Non-Cryst Solids, 2000, 270: 103–114.
- [23] KÖSTER U, MEINHARDT J, ROOS S, LIEBERTZ H. Formation of quasicrystals in bulk glass forming Zr–Cu–Ni–Al alloys [J]. Appl Phys Lett, 1996, 69: 179–181.
- [24] LU Z P, LIU C T. Glass formation criterion for various glass-forming systems [J]. Phys Rev Lett, 2003, 91: 115505.
- [25] SCHERER G W. Editorial comments on a paper by Gordon S. Fulcher [J]. J Am Ceram Soc, 1992, 75: 1060–1062.
- [26] ANGELL C A, SICHINA W. Thermodynamics of the glass transition: Empirical aspects [J]. Annals of the New York Academy of Sciences, 1976, 279: 53–62.
- [27] BÖHMER R, ANGELL C A. Correlations of the nonexponentiality and state dependence of mechanical relaxations with bond connectivity in Ge–As–Se supercooled liquids [J]. Phys Rev B, 1992, 45: 10091–10094.
- [28] ITO K, MOYNIHAN C T, ANGELL C A. Thermodynamic determination of fragility in liquids and a fragile-to-strong liquid transition in water [J]. Nature, 1999, 398: 492–495.
- [29] ZHAO Z F, ZHAO D Q, WANG W H. A highly glass-forming alloy with low glass transition temperature [J]. Appl Phys Lett, 2003, 82: 4699–4702.
- [30] BRUNING R, SAMWER K. Glass transition on long time scales [J]. Phys Rev B, 1992, 46: 11318–11322.
- [31] BUSCH R, BAKKE E, JOHNSON W L. Viscosity of the supercooled liquid and relaxation at the glass transition of the Zr_{46.75}Ti_{8.25}Cu_{7.5}Ni₁₀Be_{27.5} bulk metallic glass forming alloy [J]. Acta Mater, 1998, 46: 4725–4732.
- [32] SHADOWSPEAKER L, BUSCH R. On the fragility of Nb–Ni-based and Zr-based bulk metallic glasses [J]. Appl Phys Lett, 2004, 85: 2508–2511.
- [33] BORREGO J M, CONDE A, ROTH S, ECKERT J. Glass-forming ability and soft magnetic properties of FeCoSiAlGaPCB amorphous alloys [J]. J Appl Phys, 2002, 92: 2073–2078.
- [34] YU B, BAI H Y. Excellent glass-forming ability in simple Cu₅₀Zr₅₀-based alloys [J]. J Non-Cryst Solids, 2005, 351: 1328–1332.
- [35] LIU Z Q, LI R, LIU G, SU W H, WANG H, LI R, SHI M J, LUO X K, WU G J, ZHANG T. Microstructural tailoring and improvement of mechanical properties in CuZr-based bulk metallic glass composites [J]. Acta Mater, 2012, 60: 3128–3139.
- [36] CAI A H, XIONG X, LIU Y, LI J H, AN W K, LUO Y. Characteristics of near-eutectic and off-eutectic Zr–Al–Ni–Cu glass forming alloys [J]. Mater Sci Eng A, 2009, 516: 100–102.

具有低脆性参数的 Zr–Al–Ni–Cu 玻璃形成合金

安伟科¹, 熊翔², 刘咏², 蔡安辉^{1,2}, 周果君¹, 罗云¹, 李铁林¹, 李小松¹

1. 湖南理工学院 机械工程学院, 岳阳 414006; 2. 中南大学 粉末冶金国家重点实验室, 长沙 410083

摘要: 采用铜模铸造法制备出一系列 Zr–Al–Ni–Cu 块体非晶合金, 其脆性参数值分别采用 Arrhenius 和 Vogel–Fulcher–Tammann (VFT)方法进行计算。结果表明, 这些非晶合金具有低的脆性参数值, 其原因可能与网络状的微观结构有关。另外, Zr–Al–Ni–Cu 合金的脆性参数值可以通过 Zr 含量进行调整, 当 Zr 含量接近 54%(摩尔分数)时, Zr–Al–Ni–Cu 合金, 即 Zr₅₄Al₁₃Cu₁₈Ni₁₅ 合金的脆性参数值最小, 约为 13。

关键词: Zr–Al–Ni–Cu 合金; 非晶合金; 脆性

(Edited by Xiang-qun LI)